

# Sound absorption and form retention of newly developed heat-insulating/acoustic material

Satoshi Fukuta · Miyoko Nishizawa · Yasuo Takasu · Yukinobu Ohta · Tatsunori Mori · Mariko Yamasaki · Yasutoshi Sasaki

Received: 4 July 2011 / Published online: 27 March 2012  
© Springer-Verlag 2012

**Abstract** A wooden mat to be used as heat-insulating/acoustic material was developed using wood shavings in their raw curled flake form as the primary material. This report discusses the influences of fabrication conditions on sound absorption and form retention. The results showed that the form retention was increased with kenaf composition. However, the normal incidence absorption coefficient decreased with increasing kenaf composition and improved with increasing shavings composition. The increase of air-flow resistivity was shown as the reason. Moreover, element's internal loss of solid-borne sound transmission and the influences of various acoustic parameters that the shape of the element brought were considered as the reason. Sound absorption coefficient in a reverberation room was measured under optimum fabrication conditions, and the performance of the mat was found to be approximately equal to that of glass wool.

## Schallabsorption und Formbeständigkeit eines neu entwickelten Wärme- und Schalldämmmaterials

**Zusammenfassung** Entwickelt wurde eine Holzmatte zur Verwendung als Wärme- und Schalldämmmaterial. Dafür

wurden als Hauptmaterial natürlich gekrümmte Hobelspäne verwendet. In dieser Studie wird der Einfluss der Herstellungsbedingungen auf die Schallabsorption und Formbeständigkeit beschrieben. Die Ergebnisse zeigten, dass die Formbeständigkeit mit zunehmendem Anteil an Kenafbast zunahm. Jedoch nahm die Dämmwirkung mit zunehmendem Kenafanteil ab und mit zunehmendem Hobelspananteil zu. Als Grund dafür wurde die Zunahme des Luftstromwiderstandes festgestellt. Außerdem wurde die geringere Körperschallübertragung sowie von der Spanform abhängige Akustikparameter als Grund hierfür angesehen. Es wurde der Schallabsorptionsgrad in einem Hallraum unter optimalen Herstellungsbedingungen gemessen und es wurde gezeigt, dass die Eigenschaften der Matte mit denjenigen von Glaswolle vergleichbar sind.

## 1 Introduction

Product manufacturing in recent years requires the reduction of environmental burden throughout the product life cycle from manufacturing to disposal processes, and LCA (Life Cycle Assessment), regarded as a guideline for manufacturing, is now being recognized as one of the parameters for measuring product performance. Given such a social background, a wooden material is considered to possess great potential for the future depending on its usage.

For this reason, heat-insulating/acoustic material has been developed using wood as the primary material. A sample wooden mat (hereafter “mat”) was made using wood shavings arising from the manufacture of supports and other structural materials for homes, in their original curled flake form. The mat is characterized by the application of bicomponent fibers as binding component to mold the materials. The molding mat is flexible and low in density, yet has form

S. Fukuta (✉) · M. Nishizawa · Y. Takasu  
Aichi Industrial Technology Institute, 1-157-1 Onda-cho, Kariya,  
Aichi 448-0013, Japan  
e-mail: [fukuta@aichi-inst.jp](mailto:fukuta@aichi-inst.jp)

Y. Ohta  
Aichi Prefectural Government, 3-1-2 Sannomaru Naka-ku,  
Nagoya-city, Aichi 460-8501, Japan

T. Mori · M. Yamasaki · Y. Sasaki  
Graduate School of Bioagricultural Science, Nagoya University  
Furo-cho, Chikusa-ku, Nagoya-city, Aichi 464-8601, Japan

**Table 1** Mat fabrication conditions  
**Tab. 1**  
 Herstellungsbedingungen der Matten

Composition	Combination rate (%)	Density (g/cm <sup>3</sup> )	Thickness (mm)
	( Wood shavings : Kenaf : Bicomponent fibers )		
A	(0 : 95 : 5)		
B	(25 : 70 : 5)	0.03	25
C	(47 : 47 : 5)	λ	28
D	(70 : 25 : 5)	0.08	50
E	(95 : 0 : 5)		

retention that allows it to be used inside walls. The mat was also confirmed to have insulation/sound absorption equivalent to that of glass wool (Fukuta et al. 2010). This form retention showed a tendency to improve with the inclusion of long fibers of kenaf bast (hereafter “kenaf”) as the secondary material. However, this addition affected the sound absorption of the mat.

Sound absorption of wood and wooden material was first discussed by Watanabe et al. (1967), Takahashi et al. (1973), and others. Sound absorption of commercial insulation board, cemented excelsior board, and others became publicly known in the field of architecture. In recent years, there have been studies investigating the use of barks to replicate the performance of glass wool (Nakaoka and Ishihara 2009). Wassilieff (1996) attempted to apply a simulation model to predict the sound absorption of wood fibers and shavings. However, there are no quantitative reports using specimens of molding mat on the detailed sample of development stage. Since Wassilieff used fine shavings sifted through a 2 mm mesh, his study is different from the present study with respect to the element form.

This report investigated the influence of element composition on form retention and sound absorption of the mat by changing the mixing ratio of shavings and kenaf. In particular, the mechanism of sound absorption was considered by examining acoustic parameters such as element form and airflow resistivity to investigate the direction for application of wood fibers/materials.

## 2 Materials and methods

### 2.1 Specimens

Specimens are wooden mats made from shavings, kenaf, and bicomponent fibers. Shavings were obtained from Japanese cedar (*Cryptomeria japonica*) having an air-dry density of 0.35–0.40 g/cm<sup>3</sup> using an automatic planing machine. They were used without sorting by size. As for kenaf, 80-mm-long spread fibers from kenaf bast were used. The authors used ESC (ES Fibervisions) composed of a polypropylene core with a polyethylene sheath having a fineness of 2.2 dtex and a length of 5 mm as the bicomponent fibers.

These basic materials were fabricated according to the method described in a past report (Fukuta et al. 2010), fibrous materials such as kenaf and bicomponent fibers were spread applying a modified dust collector with an air blower and a chamber, and then wood shavings were mixed together through the same system. Bicomponent fibers are composed of two resins of different properties, by heating to a temperature at which only the sheath melts, fibers weld together. Bicomponent fibers also connect shavings and kenaf in the mesh structure of bicomponent fibers. Thermoforming process used this bicomponent fiber weld mechanism. Although it was efficient and practical to use heat through dryer for the thermoforming, a conventional oven dryer had been used for heating the mixture in this study. The heating temperature was set to 160 °C, for a heating time of 2 h.

It was discovered that the inclusion of kenaf improves form retention of the mat, but has an influence on its sound absorption. Therefore, specimens were produced having different compositions shown in Table 1 in order to examine the influence of element composition ratio on form retention and sound absorption.

### 2.2 Evaluation of form retention

To estimate form retention of the mats, its self-support capability was evaluated using Young’s modulus and its mass retention rate using repeat free-fall test as previously reported. Young’s modulus ( $E$ ) was calculated using Eq. (1) by measuring the deflection of samples when supported as a cantilever beam using a laser displacement meter (Fig. 1). The test piece dimensions were set to 310 mm by 100 mm by 28 mm; samples were fixed at a distance of 110 mm in the length direction from the tip, and a certain load ( $P$ ) was applied to the other tip, allowing it to deflect freely. Then, the deflection from the anchor was measured at regular intervals using a laser deflection meter. Since the result showed deformation similar to a free deflection curve, an average value of the Young’s modulus was calculated for each measuring position on the cantilever for each test piece. There were three test pieces.

$$E = \frac{q}{24I\delta}x^2(6l^2 - 4lx + x^2) + \frac{P}{6I\delta}(3lx^2 - x^3) \text{ (Pa)} \quad (1)$$

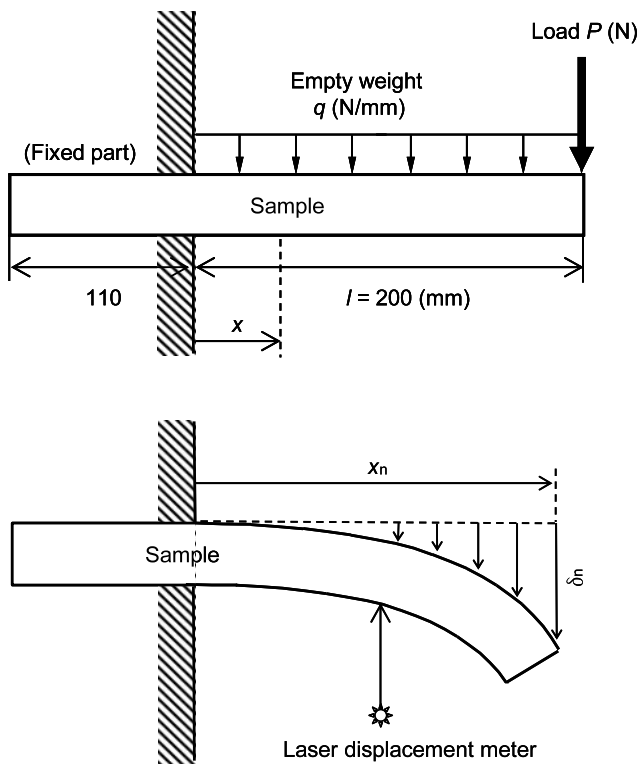


**Fig. 1** Calculation of Young’s modulus with measured deflection  
**Abb. 1** Berechnung des Elastizitätsmoduls über die gemessene Durchbiegung

where  $q$  = load per unit length (N/mm);  $I$  = second moment of section ( $\text{mm}^4$ );  $\delta$  = deflection amount (mm);  $x$  = distance from the fulcrum (mm);  $l$  = beam length (mm); and  $P$  = load applied to the tip (N).

For the repeat free-fall test, the test piece dimensions were set to 310 mm by 310 mm by 25 mm; when dropped in free fall from a height of 7.5 m, the mass ( $W_n$ ) of the largest piece remaining undestroyed was measured, and the mass retention rate was obtained over 12 repeats. There were three test pieces.

Statistical analyses were carried out to Young’s modulus and mass retention rate in each density according to the Bonferroni multiple comparison test (Ott and Longnecker 2001).

### 2.3 Sound absorption characteristics

The normal incidence absorption coefficient and the sound absorption coefficient in a reverberation room were measured to identify sound absorption. The airflow resistivity was also measured to consider these characteristics.

To calculate the normal incidence absorption coefficient ( $\alpha_0$ ), the measurement system of WinZac MTX Version 3.1.0 (Nittobo Acoustic Engineering Co., Ltd.) (Fig. 2), which conformed to ISO 10534-2 (ISO 1998) was used. This system generates noise from the edge of acoustic tube

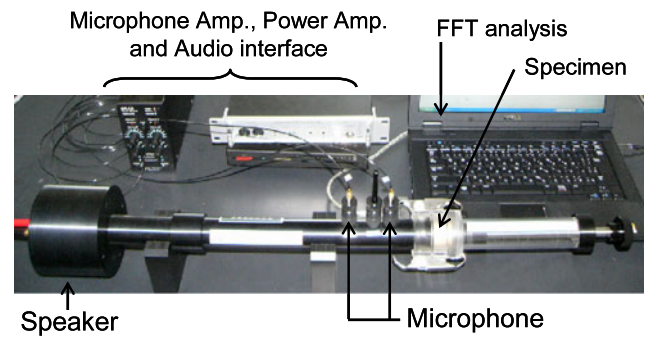


**Fig. 2** Normal incidence absorption coefficient measurement system  
**Abb. 2** Messsystem zur Bestimmung des Schallabsorptionsgrades

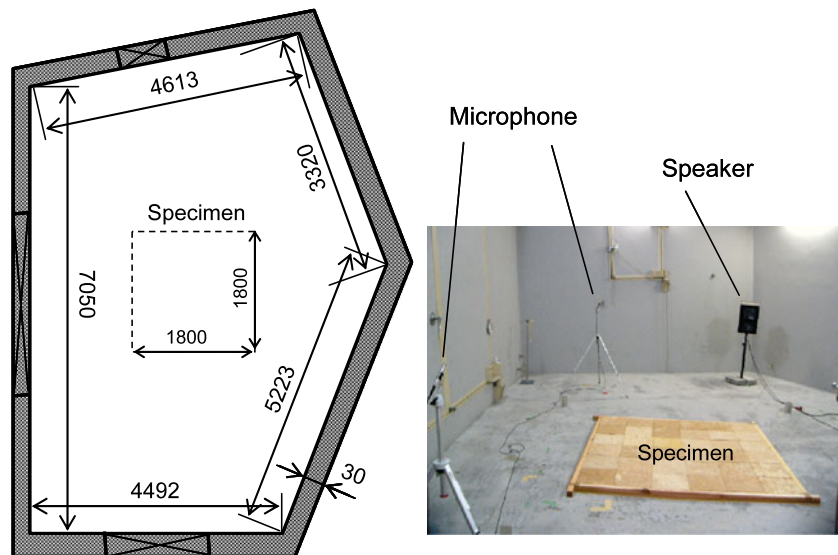
toward the test piece placed on the other edge and evaluates the absorbency of one-way incident sound. A test piece 30 mm in diameter was cut from a 25-mm-thick mat and its density was measured simultaneously. Test pieces of glass wool of densities 0.096  $\text{g}/\text{cm}^3$  (GW96) and 0.032  $\text{g}/\text{cm}^3$  (GW32), as well as closed-cell polystyrene foam (SF28) of density 0.028  $\text{g}/\text{cm}^3$  were used for comparison. The air layer at the back of the specimen was set to 0 mm.

The sound absorption coefficient in the reverberation room ( $\alpha_s$ ) was measured according to ISO 354 (ISO 2003). However, the area of the specimen was set to 3.4  $\text{m}^2$  for this study. The reverberation room and the condition in which the specimen was placed are shown in Fig. 3. The reverberation room is heptahedron with its floor surface slanted with respect to its ceiling. The room has a capacity of 195  $\text{m}^3$  and interior surface area of 201  $\text{m}^2$ . The specimen was 50 mm thick. This test evaluates the sound absorption of the test piece by measuring the reverberation time after stopping the sound generated inside the room. This testing method allows to estimate the performance characteristics of the mat based on actual usage patterns by evaluating the absorption of incident sound from random directions.

The airflow resistivity was measured using an air permeability tester (KES-F8-AP1, Kato Tech Co., Ltd.) with a sample 89.5 mm in diameter cut from a 50-mm-thick mat. The airflow resistivity is calculated from the difference in pressure across the sample when air is ventilated through its thickness at a certain speed. The airflow resistivity per unit thickness  $r_0$   $\text{N s}/\text{m}^4$  was calculated using the following equation. The tester measured the pressure difference  $\Delta P$   $\text{N}/\text{m}^2$  across the sample as well as the ventilation volume  $V$   $\text{m}^3/(\text{m}^2 \text{ s})$ , and the ventilation resistivity  $r$   $\text{N s}/\text{m}^3$  was calculated by Eq. (2). This is same as the airflow resistivity obtained from dividing the pressure difference across the sample  $\Delta P$   $\text{N}/\text{m}^2$  by flow velocity  $v$   $\text{m}/\text{s}$ . Therefore, the airflow resistivity  $r_0$   $\text{N s}/\text{m}^4$  was calculated by dividing it by the sample thickness  $t$   $\text{m}$ , as indicated in Eq. (3). With this tester, the flow velocity  $v$  was  $0.4 \times 10^{-2}$   $\text{m}/\text{s}$ .

$$r = \frac{\Delta P}{V} = \frac{\Delta P}{v} \quad (\text{N s}/\text{m}^3) \tag{2}$$

**Fig. 3** Reverberation room and specimen in reverberation room  
**Abb. 3** Hallraum und Prüfkörper im Hallraum



$$r_0 = \frac{r}{t} \quad (\text{N s/m}^4) \quad (3)$$

The porosity  $\phi$  represents the proportion of void in the volume of the mat, which is calculated by Eq. (4) using the element density  $\rho_e$  and mat bulk density  $\rho$ . Cell pores of wood and kenaf have no effect on acoustic property of the mat. Thus, for the calculation, not the true density of wood but the average density of Japanese cedar, which was  $0.375 \text{ g/cm}^3$ , was used as the density of shavings ( $\rho_e$ ). The kenaf density ( $\rho_e$ ) of  $1.216 \text{ g/cm}^3$  was calculated using the proportion of cell pores obtained from the observation image of kenaf fiber cross section (Suzuki et al. 2005) and the true density of cellulosic natural fibers that is  $1.5 \text{ g/cm}^3$ .

$$\phi = 1 - \frac{\rho}{\rho_e} \quad (4)$$

where  $\rho$  = mat bulk density ( $\text{g/cm}^3$ );  $\rho_e$  = element density ( $\text{g/cm}^3$ ).

### 3 Results and discussion

#### 3.1 Form retention

Figure 4 shows the Young's modulus of molding mats. The empty weight of the cantilever section increased as the density became higher, but Young's modulus was greater at higher density for all compositions. This is because the bonds between elements also become denser. Moreover, Young's modulus improved as the composition of long-fiber kenaf increased. This is considered to be due to the mutual connection between wood shavings that are supported as they entangled themselves with kenaf. Young's modulus was expected to improve in proportion to the kenaf composition rate and notable improvements were confirmed up to

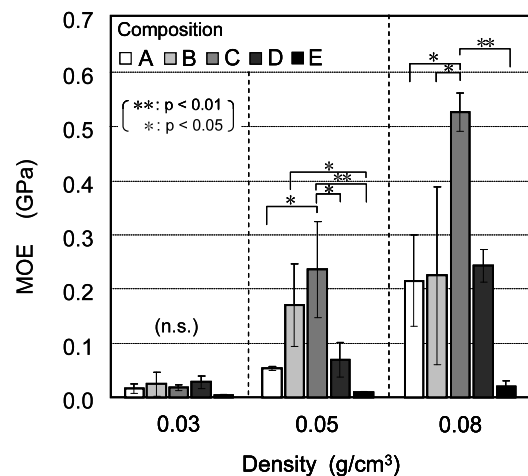


**Fig. 4** Young's modulus of the mat  
**Abb. 4** Elastizitätsmoduln der Matten

a certain composition (composition C). For higher compositions (composition B, A), however, Young's modulus decreased and its values varied considerably under the high-density condition. This is due to the influence of spreading technique used in this study, which caused inhomogeneous forming of mixed specimens in the formwork. Composition A and B have spreading kenaf fibers that have flocculated to form extremely large clumps, causing partial discontinuation of the molding mat. It is considered that it is impossible to avoid these problems on kenaf-rich combination rate. To avoid these problems, a different spreading technique must be used for the condition. Therefore, when considering practical applications under this production technique, composition C or D is more appropriate.

Figure 5 shows the mass retention in the repeat free-fall test. Scatterings of fine wood shavings and powder from test pieces resulted in small reductions in mass. Large re-

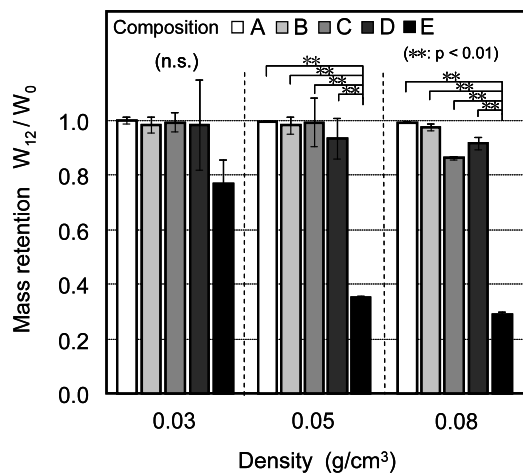


**Fig. 5** Mass retention rate after repeat free-fall test  
**Abb. 5** Massebeständigkeit nach wiederholten Fallversuchen

ductions in mass were due to the partial destruction of the test piece. In this falling test, the destruction of test piece was controlled and good mass retention was confirmed at a kenaf composition of 25 % (composition D) under any density condition. The mass retention improved slightly as the proportion of kenaf increased. These trends can be explained by the mutual connection between elements as seen in the observations for Young's modulus and reduction in the absolute quantity of shavings, which are vulnerable to scattering. A difference from Young's modulus was that the mass retention did not decrease for composition A and B with high kenaf composition. In other words, formability of composition A and B was not considered unstable to break down with drop impact. When comparing the effect of density, the mass retention decreased with increasing density of test pieces. This is considered to be due to the impact of acceleration which increases in proportion to mass.

### 3.2 Sound absorption characteristics

Figure 6 shows the results for normal incidence absorption coefficient. It indicates the influence of mixing ratio on the absorption coefficient in each density condition. The results for GW96, GW32, and SF28 are also indicated in the figures. In general, the performance of the fibrous porous material is determined by density and thickness. As demonstrated in the results for GW96 and GW32, sound absorption frequency tended to shift to the low-frequency side with increased density. Mutual comparison of Fig. 6(a)–(c) demonstrates that the sample mat also showed a similar tendency as the peak frequency shifted to the low-frequency side with density increase. Moreover, the absolute value at the peak tended to increase in response to density. When comparing the mixing ratios, sound absorption improved as the shavings composition increased. When comparing the mat, ex-

cept for composition A, with GW32 and GW96 in the mid-low frequency range up to 2 kHz, the performance of the mat of density 0.06 g/cm<sup>3</sup> (Fig. 6(b)) was similar to or better than that of GW32, and performance of the mat of density 0.08 g/cm<sup>3</sup> (Fig. 6(c)) approximately equivalent to that of GW96. Specimens of composition A and B with higher density (Fig. 6(d)) were prepared and measured, and the result showed improvement for composition A in all frequency ranges, but no difference was observed between the result for densities of 0.10 g/cm<sup>3</sup> and 0.11 g/cm<sup>3</sup>. Composition B showed no significant improvement for density above 0.08 g/cm<sup>3</sup>. Therefore, these results are assumed to be the maximum under the given mixing conditions. For composition C–E, no high-density specimens could be prepared using this processing method because spring-back was caused after thermoforming, as described in a previous report (Fukuta et al. 2010).

One of the characteristics of these mats in comparison to glass wool is the decline of absorption rate that was evident in Fig. 6(b) and (c) for the frequency range of 2–4 kHz, and the ratio declined further with the increase in shaving composition. Generally, other materials such as glass wool show this decline slightly, which is considered to be due to the sound reflection on the specimen surface. In other words, partial decline in absorption coefficient is observed as a result of the mutual enhancement of the sound reflected from specimen surface and back surface wall. Since the mats have shavings in flake form exposed on the surface, it is anticipated that the decline in absorption coefficient was caused by larger composition of shavings, which led to greater reflection. On the contrary, the influence of the interference with the reflected sound is considered as expressed in the performance around that frequency. As discussed in a previous case study (Nakaoka and Ishihara 2009) on wood fibers as a sound absorbing material, the element form was relatively similar to this study and a similar tendency was observed. It is therefore preferable to use a specimen with appropriate composition of kenaf for absorbing sound in the frequency range of 2–4 kHz.

To further examine the influence of mixing ratio on the absorption performance, airflow resistivity was measured and porosity was calculated for compositions A and E, which have the greatest difference in mixing ratio (Table 2). The table also includes literature data for glass wool. Airflow resistivity is a major parameter that determines absorption performance, and this value is used to simulate absorption performance of fibrous porous materials (Delany and Bazley 1970; Miki 1990). Sound absorption improves at higher airflow resistivity (Koyasu 1990), but nonporous closed-cell foam materials do not show sound absorption as shown in the result for SF28. The measurement results showed that airflow resistivity of composition E was more than twice of composition A. The authors observed the cross



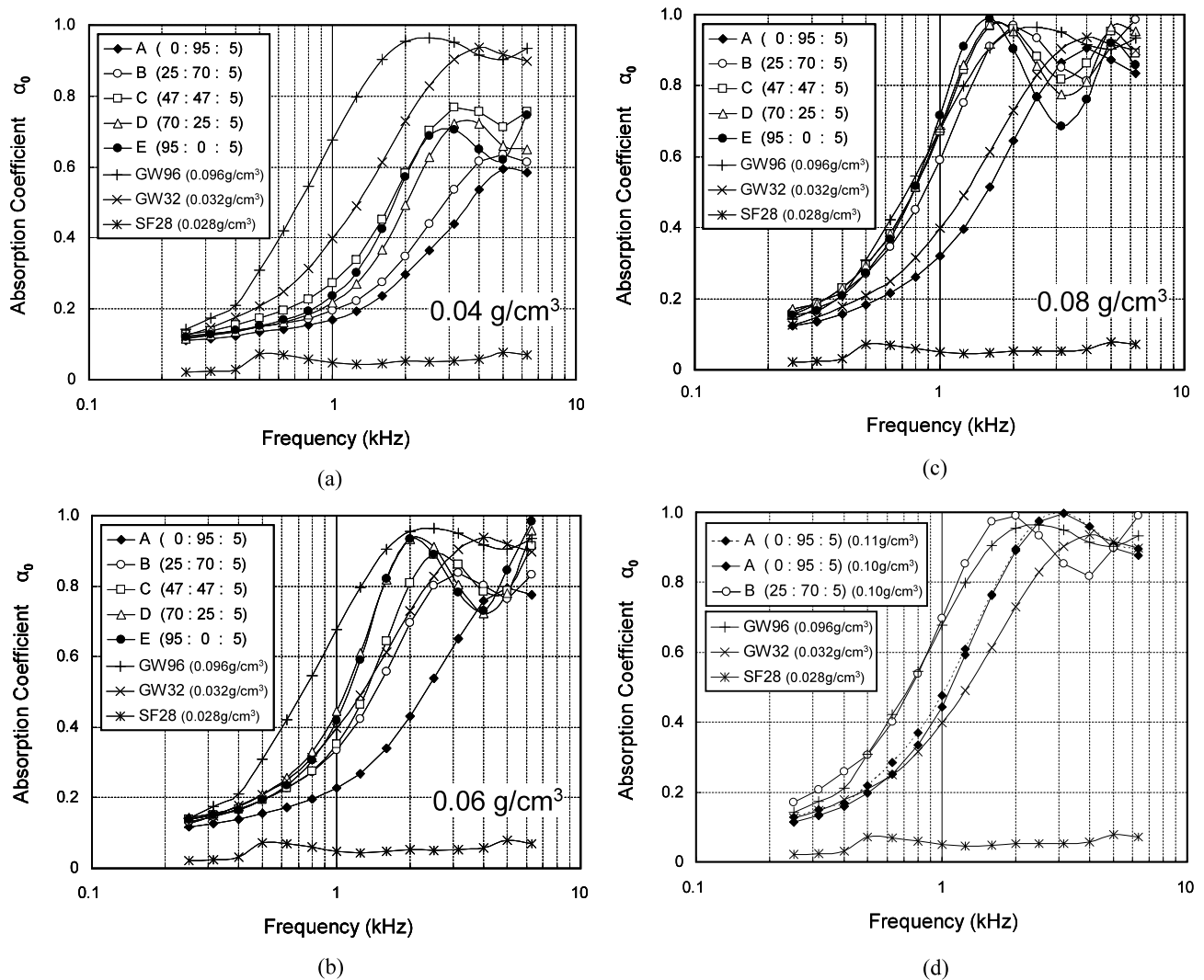


**Fig. 6** Normal incidence absorption coefficient  $\alpha_0$ . (a) 0.04 g/cm<sup>3</sup>; (b) 0.06 g/cm<sup>3</sup>; (c) 0.08 g/cm<sup>3</sup>; (d) 0.10, 0.11 g/cm<sup>3</sup>  
**Abb. 6** Schallabsorptionsgrad  $\alpha_0$ . (a) 0,04 g/cm<sup>3</sup>; (b) 0,06 g/cm<sup>3</sup>; (c) 0,08 g/cm<sup>3</sup>; (d) 0,10; 0,11 g/cm<sup>3</sup>

section of the two specimens, which are shown in Fig. 7. Composition E had its shavings in curled, crushed, or flat flake forms, and the shavings were piled in the thickness direction. As illustrated in the figure, the airflow pathway for composition E is more complicated than that for composition A, causing greater resistivity for composition E. The increase of airflow resistivity is considered to be one of the reasons for improvement of sound absorption at higher shavings compositions. On the other hand, as indicated in Table 2, it is reported that a glass wool of density 0.08 g/cm<sup>3</sup> has airflow resistivity of approximately 30000 N s/m<sup>4</sup> and 97 % porosity (Nakagawa et al. 1994), indicating greater airflow resistivity at low-density than the mats. Therefore, it was anticipated that the mat has parameters other than airflow resistivity that contribute to sound absorption. When porosities are compared, composition E has a porosity of 74.7 %, which is lower than that of glass wool and composi-

**Table 2** Airflow resistivity and porosity

**Tab. 2** Luftstromwiderstand und Porosität

Composition	Density $\rho$ (g/cm <sup>3</sup> )	Airflow resistivity $r_0$ (N s/m <sup>4</sup> )	Porosity $\phi$ (%)
A	0.085	8810 (S.D. 560)	93.0
E	0.088	21190 (S.D. 1800)	74.7
(Glass wool) <sup>a</sup>	0.080	30000	97.0

<sup>a</sup>Nakagawa et al. (1994)

tion A, and therefore the influence of elements in itself must be considered for composition E. In one word, viscoelastic character of the elements and other acoustic parameters except airflow resistivity are considered to affect sound absorption. For such materials, various parameters such as shear modulus, internal loss, and Poisson's ratio were considered

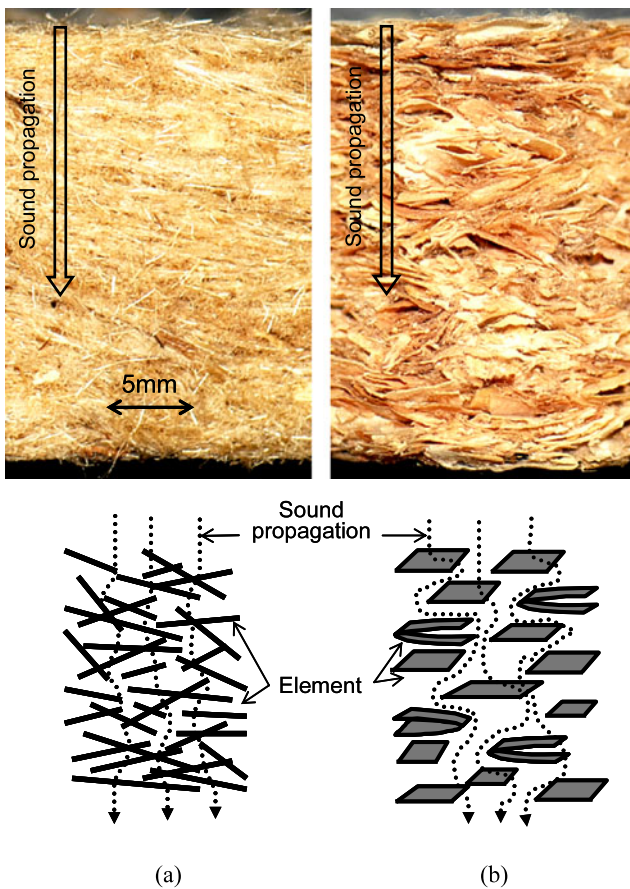


**Fig. 7** Cross-section and diagram of specimen (a) Composition A (Wood shavings : Kenaf : B.F. = 0 : 95 : 5). (b) Composition E (Wood shavings : Kenaf : B.F. = 95 : 0 : 5)  
**Abb. 7** Querschnitt und Schema der Prüfkörper (a) Variante A (Hobelspäne : Kenaf : B.F. = 0 : 95 : 5); (b) Variante E (Hobelspäne : Kenaf : B.F. = 95 : 0 : 5)

for viscoelastic character. And tortuosity, viscous characteristic length, and thermal characteristic length were considered for acoustic parameters while constructing a simulation model (Attenborough 1993; Johnson et al. 1987; Allard and Atalla 2009). Among these parameters, internal loss, tortuosity, and viscous characteristic length mainly affect the mat performance. Internal loss is the element’s internal loss of solid-borne sound transmission, and this affects the sound absorption in materials such as urethane foam. Given the porosity of the mat, this effect is considered to be significant. Tortuosity shows quantified value of change in apparent sound velocity caused by indirect sound propagation through the pores of specimens. The diagram of composition E in Fig. 7 illustrates the pathway of a sound wave, which yields a higher tortuosity than composition A. Viscous characteristic length shows quantified value of the influence of air viscosity resulting from the complexity of the internal structure. As illustrated in the diagram, composition E has airflow path with flakes piled close to each other, and the influence of air viscosity is considerable, which is higher

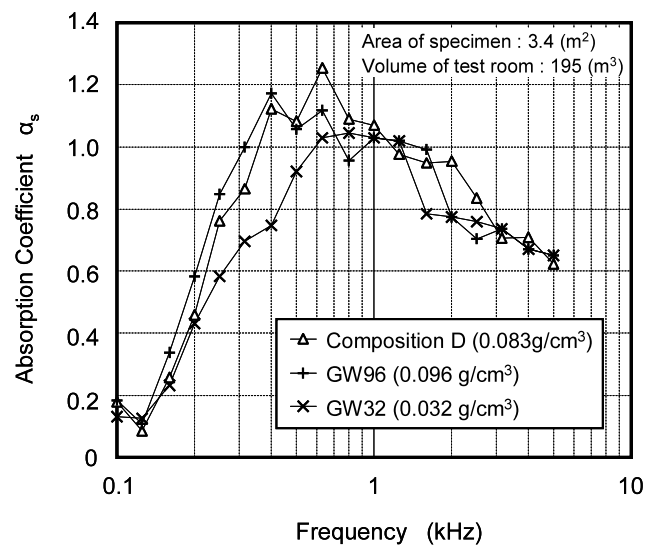


**Fig. 8** Sound absorption coefficient in a reverberation room  $\alpha_s$   
**Abb. 8** Schallabsorptionsgrad im Hallraum  $\alpha_s$

than that for composition A. In order to clarify the mechanism that shaving composition causes sound absorbency, the factors need to be specified through various studies in the future.

Next is the result of sound absorption coefficient in a reverberation room, which is shown in Fig. 8. This test compared composition D, which showed relatively favorable results of normal incidence absorption coefficient, with GW96 and GW32. When comparing three specimens under the same condition, composition D and GW96 showed higher sound absorption than GW23 in the mid-low frequency around 400 kHz. Absorption of composition D and GW96 were approximately equal with a slight difference depending on the frequency range. This method of using reverberation room had no local decline in sound absorption, which is seen in the case of normal incidence absorption. This is considered to be due to the reduced enhancement (resonance) with sound waves entering in the specimen from various directions.

#### 4 Conclusion

A sample wooden mat to be used as heat-insulating/acoustic materials was made using wood shavings in their raw curled flake form as the primary material. This report discusses the influence of mixing ratio of wood shavings and kenaf component on form retention and sound absorption. To estimate the form retention of the mat, the authors evaluated Young’s modulus and mass retention with repeat free-fall test. The results showed that Young’s modulus peaked at kenaf composition of 50 %, and satisfactory mass retention was confirmed in the repeat free-fall test with 25 % kenaf composition. The normal incidence absorption coefficient showed

a shift of absorption frequency toward low-frequency side and improvement in absorption rate with increased density. When comparing the influence of mixing ratio, absorption performance decreased with increased kenaf composition, and improved with increased shavings, except for a specific range of frequency. As reason for improved absorption, the increased airflow resistivity, element's internal loss of solid-borne sound transmission, and influences of various acoustic parameters caused by the form of elements was considered. When the sound absorption coefficient in a reverberation room was measured with overall optimum mixing ratio (wood shavings : kenaf : bicomponent fibers = 70 : 25 : 5), the performance of a mat of density  $0.08 \text{ g/cm}^3$  was found to be approximately equal to that of glass wool of density  $0.096 \text{ g/cm}^3$ . Now, the application of this material is also thermal insulation. The fabrication conditions and structural factors based on element's form must have influenced the thermodynamic properties like acoustic characteristics. They are under examination now, and it is planned to report them immediately.

**Acknowledgements** We extend our heartfelt gratitude to Tokushima Prefectural Industrial Technology Center for their assistance in measuring airflow resistivity.

## References

- Allard JF, Atalla N (2009) Sound propagation in porous materials having a rigid frame. In: Propagation of sound in porous media. Modeling sound absorbing materials, 2nd edn. Wiley, West Sussex, pp 73–107. Chap. 5
- Attenborough K (1993) Models for the acoustical properties of air-saturated granular media. *Acta Acoust* 1:213–226
- Delany ME, Bazley EN (1970) Acoustical properties of fibrous absorbent materials. *Appl Acoust* 3(2):105–116
- Fukuta S, Nishizawa M, Ota Y, Takasu Y, Mori T, Yamasaki M, Sasaki Y (2010) Development of low-density wooden molding mat using bicomponent fibers. *For Prod J* 60(7/8):575–581
- ISO 10534-2 (1998) Determination of sound absorption coefficient and impedance in impedance tubes—Part 2: Transfer-function method. International Organization for Standardization (ISO), Geneva
- ISO 354 (2003) Measurement of sound absorption in a reverberation room. International Organization for Standardization (ISO) Geneva
- Johnson DL, Koplic J, Dashen R (1987) Theory of dynamic permeability and tortuosity in fluid-saturated porous media. *J Fluid Mech* 176:379–402
- Koyasu M (1990) Fundamentals on sound absorption and sound absorbing materials. *Architect Acoust Noise Control* 19(3):2–7
- Miki Y (1990) Acoustical properties of porous materials—Modifications of Delany–Bazley models. *J Acoust Soc Jpn* 11(1):19–24
- Nakagawa H, Ohashi S, Ohara Y, Ogawa T, Shima H, Yamaguchi M (1994) The measurement of airflow resistance by DC method and AC method. In: Proc. inter-noise 94, Yokohama, Japan, 29–31 August 1994, pp 1943–1946. International Institute of Noise Control Engineering
- Nakaoka M, Ishihara K (2009) On sound absorption properties of bark fiber and its estimation method. *J INCE/J* 33(6):446–457
- Ott LR, Longnecker MT (2001) The analysis of covariance. In: An introduction to statistical methods and data analysis, 5th edn. Duxbury, Pacific Grove, pp 943–974. Chap 16
- Suzuki K, Kimpara I, Saito H, Funami K (2005) Cross-sectional area measurement and monofilament strength test of kenaf bast fibers. *J Soc Mater Sci Jpn* 54(8):887–894
- Takahashi A, Tanaka C, Ikegami Y, Senuma I, Iwashige H (1973) On the sound absorbing coefficient and transmission loss of wood-based materials. *Bull Faculty Agriculture Shimane Univ* 7:69–79
- Wassilief C (1996) Sound absorption of wood-based materials. *Appl Acoust* 48(4):339–356
- Watanabe H, Matsumoto T, Kinoshita N, Hayashi H (1967) Acoustical study of woods and wood products. I. On the normal absorption coefficient of wood. *Mokuzai Gakkaishi* 13(5):117–182